Simultaneous triple-radiation Mössbauer spectroscopy investigation of surface and bulk magnetic properties of Fe_3BO_6 near the Néel temperature

A. S. Kamzin and L. A. Grigor'ev

A. F. Ioffe Physicotechnical Institute, Russian Academy of Sciences, 194021 St. Petersburg, Russia
(Submitted 24 July 1993)
Zh. Eksp. Teor. Fiz. **105**, 377–391 (February 1994)

The surface and bulk magnetic properties of a macroscopic antiferromagnetic Fe_3BO_6 crystal were investigated simultaneously near the phase transition at the Néel point (T_N) in the interior of the crystal. The measurements were performed by the method of simultaneous triple-radiation Mössbauer spectroscopy, which enables the surface and bulk properties of a macroscopic crystal to be studied simultaneously. It was found that 1) the temperature $T_N(L)$ of the transition of a thin layer, located at a depth L from the surface of the crystal, into a disordered state decreases as the layer approaches the surface; 2) the paramagnetic transition at the surface is preceded by a wide interval of temperatures in which relaxational processes are observed and which becomes narrower as the distance from the surface increases; 3) near T_N there exists a nonuniform state in which the crystal is magnetically ordered in the bulk but disordered at the surface; and, 4) as the crystal is heated paramagnetic islands form on the surface of the crystal at temperatures $T \ll T_N$, and these islands spread over the surface and penetrate into the crystal as the temperature increases. Under further heating the thickness of the paramagnetic surface layer reaches a critical value and then the entire remaining volume of the crystal passes as a whole into the paramagnetic state. In the critical layer the temperature of the transition to the disordered state changes from some minimum value at the surface to T_N at the lower boundary of this critical layer.

1. INTRODUCTION

Crystal surfaces, regarded as "defects" giving rise to new magnetic structures and interesting magnetic phenomena, are now attracting a great deal of interest. The study of these phenomena has led to the creation of a new branch of solid-state physics—surface magnetism.

Practically all methods which are used for describing magnetic phenomena in unbounded samples are also employed in theoretical investigations of surfaces (see the reviews in Refs. 1–5 and the references cited there). One of the most successful approaches for describing surface effects is the phenomenological approach of Refs. 6–8. The phenomenological approach, which dates back to the Ginzburg–Landau method in the theory of superconductivity, has made it possible to describe the surface behavior of the system with the help of the surface energy, which is proportional to the square of the order parameter.[6,7] The coefficient of proportionality is an additional phenomenological parameter. As a result, the shift of the Curie temperature, the temperature dependence of the average magnetic moment, and the magnetic-moment density at the boundary were determined[6,7] and the effect of the surface energy on the thermodynamic characteristics was investigated.[9,10]

It is evident from the experimental achievements that, for example, in polycrystalline Gd(0001) the surface magnetic-ordering temperature is higher than the Curie point in the volume of the crystal.[11] A similar picture has been observed for a Tb(0001) film on a W(110) substrate.[12,13] The surface magnetization of polycrystalline Gd (Ref. 11) is different from the magnetization of an ultrathin film of Gd(0001) on a W(110) substrate.[14] The temperature dependence of the magnetization of an ultrathin film is not necessarily linear. It is a complicated function of the correlation length and the extrapolation length, characterizing the difference between the surface and bulk magnetic exchange interaction and may be identical to the temperature dependence $T^{3/2}$ in the volume of the material.[15,16]

In Ref. 17 it was shown, by the method of traditional Mössbauer spectroscopy in the γ-ray transmission geometry, that the effective magnetic field at the surface of the film is different from that in the interior of the film. In Ref. 18 it was observed, by means of emission Mössbauer spectroscopy, that the surface magnetization of a γ-Fe_2O_3 macrocrystal decreases on heating more rapidly than the bulk magnetization and the ordering of the spin magnetic moments is noncollinear at the surface and collinear in the volume. Investigations of the alloy PdFe simultaneously by the methods of Mössbauer spectroscopy with detection of the characteristic x-rays and traditional Mössbauer spectroscopy showed that the ordering temperature at the surface is 2 K lower than in the interior.[19] In Ref. 20 an antiferromagnetic Fe_3BO_6 macrocrystal was studied by Mössbauer diffraction in the usual Bragg geometry and by conventional Mössbauer spectroscopy, and it was found that the surface spectra acquire a relaxational form at temperatures 8.5 K below the Néel point, while the volume spectra retain their Zeeman structure.

The overwhelming majority of experimental methods is employed for studying surface properties of thin or ul-

 1063-7761/94/020200-08$10.00

trathin films. Difficulties arise in comparing and interpreting the experimental results, because the experimenters often obtain either indirect data or data on different properties of the surface and interior of a bulk crystal that cannot be compared directly.

In order to understand the nature of surface phenomena and to determine the connection between surface and bulk effects the surface properties of macroscopic crystals must be studied with respect to the bulk properties. However, virtually no experimental investigations of this kind have been performed, because the existing methods for studying the surface of three-dimensional objects either make it virtually impossible to distinguish signals from the surface and the interior of the object or they are employed to investigate quite thick surface layers whose properties approach those in the bulk crystal.

In the present paper we present the results of simultaneous experimental investigations of the surface and bulk magnetic properties of Fe_3BO_6 crystals near the phase transition at the Néel point. The measurements were performed by the method of simultaneous triple radiation Mössbauer spectroscopy. This method enables studying simultaneously the properties of a surface layer with a thickness of hundreds of angstroms and of the interior of a bulk sample under the same conditions.

2. OBJECT OF INVESTIGATION AND EXPERIMENTAL PROCEDURE

An Fe_3BO_6 crystal belonging to the orthorhombic system was chosen for the investigations.[21] The magnetic structure of Fe_3BO_6 consists of four magnetic sublattices, formed by iron ions occupying two nonequivalent sites $8d$ and $4c$ at octahedral positions.[21] There are half as many $4c$ iron ions as $8d$ ions. At temperatures below the Néel point $T_N=507.7$ K for the volume of the crystal these four sublattices form two antiferromagnetic $8d$ and $4c$ sublattices. A spin-reorientation phase transition is observed in Fe_3BO_6 near $T_R\approx 415$ K.[22,23]

The magnetic properties of Fe_3BO_6, and especially phase transitions at the spin-reorientation point as well as at the Néel temperature, have been thoroughly investigated. It has been shown that spin reorientation of the type $G_zF_x \leftrightarrow G_xF_z$ at 415 K occurs in a narrow temperature interval (less than 1 K) (Ref. 22) as a first-order phase transition and is accompanied by the formation of an intermediate state.[24,25] Mössbauer investigations of a spin-reorientation phase transition at the surface and in the interior of Fe_3BO_6 macrocrystals simultaneously have shown[26] that the temperatures of this transition at the surface and in the volume of the crystal are identical, but the orientations of the spin magnetic moments are different.

One other spin-reorientation phase transition has been observed[27] in Fe_3BO_6 at 490 K. Its existence was confirmed in Ref. 28. It was found that as the temperature increases, at temperatures $\approx$490 K the magnetic moments of one antiferromagnetic sublattice ($4c$) turn continuously, while the orientation of the moments of the other sublattice ($8d$) remains the same right up to T_N. Such an orientational transition had not been previously observed in magnetic materials.

The critical exponents of Fe_3BO_6 crystals were determined in Refs. 28–30. Splitting of the critical exponents for nonequivalent Fe_3BO_6 sublattices was observed in Ref. 30. Although this effect is refuted in Ref. 28, it not only agrees with the theory of Ref. 31 but it is also confirmed by measurements performed on other objects.[32]

In the present work we chose for our investigations about 120 μm thick single-crystalline plates, obtained by the method of spontaneous crystallization from solution in a melt. The crystallographic a axis was oriented perpendicular to the surface of the plate. The surface of the single crystals was prepared by two methods: 1) mechanical polishing with fine polishing powders and light etchants and 2) chemical polishing in a 1:1 room-temperature mixture of H_3PO_4 and H_2SO_4 acids for $\sim$50 h. It should be noted that reproducible experimental results were obtained only in the second case.

In this work we employed the method of simultaneous γ-ray, x-ray, and electron Mössbauer spectroscopy,[33] known abroad as simultaneous triple-radiation Mössbauer spectroscopy (STRMS). This method enables studying simultaneously the surface and interior properties of macroscopic crystals. The crux of the method is that the Mössbauer spectra for the three types of radiations, whose ranges in the material are different, are recorded simultaneously: γ-rays, characteristic x-rays, as well as conversion and Auger electrons (secondary electrons). Thus information about the state of both surface and interior of the bulk crystal is extracted simultaneously.

A block diagram of the Mössbauer spectrometer employed in this work is displayed in Fig. 1. The proportional counters Γ, X, and E of a universal detector[34] record the γ-rays, secondary x-rays, and secondary electrons, respectively. The signals from the counters are fed, through their own amplification (A) and discrimination (D) channels, into the spectrum accumulators (Ac). The sample (S) is placed on a heater (H). The temperature is maintained constant with an accuracy of better than 0.2 K. A generator (G) determines the motion of the γ-ray source on a vibrator (V). The motion of the Mössbauer source is adjusted through two channels: The first channel consists of a conventional negative-feedback circuit. In the second channel the difference between a reference signal and the real signal of the motion is measured automatically, the difference is analyzed by a computer, and a correction signal is fed into the system controlling the motion.[35] Compared to existing spectrometers, the additional correction channel improved the linearity of the motion of the Doppler modulator by almost an order of magnitude. The spectrometer is controlled by a computer in the dialog mode.

A new step in the development of the method of Mössbauer spectroscopy was the study of surface properties layer by layer—depth-selective conversion electron Mössbauer spectroscopy. It is important that in this method the analysis is performed without damaging the sample. The method is based on the fact that the energy of an electron exiting the sample depends on the depth from which this

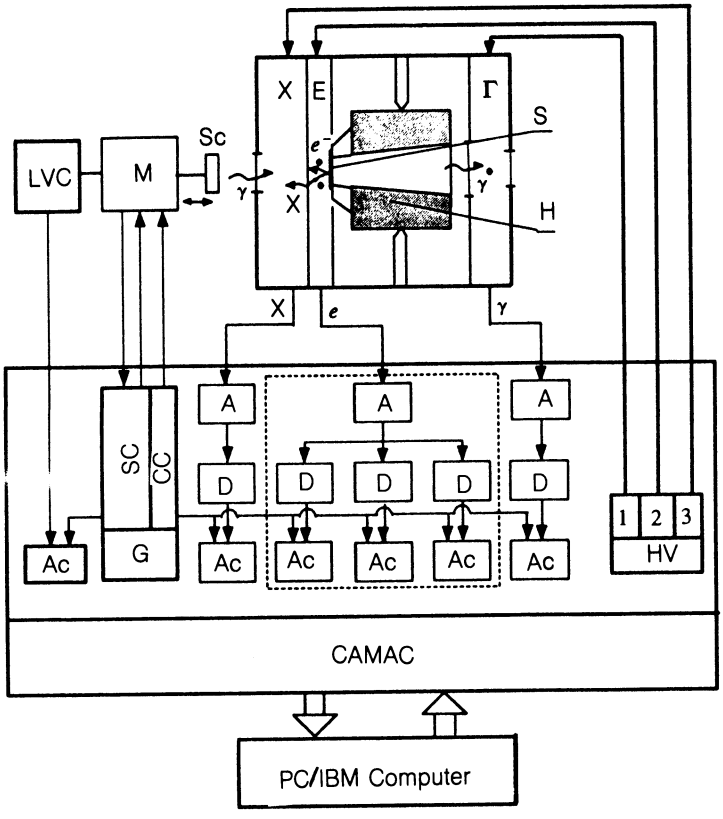

FIG. 1. Block diagram of the simultaneous triple radiation Mössbauer spectrometer: Sc—γ-ray source; S—experimental sample; H—heater; X, E, and Γ—proportional x-ray, electron, and γ-ray detectors, respectively; M—Doppler modulator; G—motion generator; SC and CC—standard and computer correction of the motion signal, respectively; LVC—laser velocity calibrator; A—amplifiers; D—discriminators; Ac—accumulators; HV—high-voltage units.

electron is emitted. The properties of a thin layer, located at a definite depth from the surface of the crystal can be investigated by recording electrons in a definite energy group and by taking into consideration the probability that the electrons reach the surface of the crystal.

Improvements to the chamber E (see Fig. 1), recording the conversion and Auger electrons, in the universal detector made it possible to select (by decreasing the anode thickness and the anode-sample distance) secondary electrons by energy with the help of a proportional detector.[36] The accuracy with which the location and thickness of the layer are determined using a proportional detector is not high compared to electrostatic or magnetic energy analyzers. However, the high transmission of a simple and inexpensive proportional detector, having adequate energy resolution, combined with mathematical analysis of the experimental spectra[37] makes it possible to obtain quite accurate information from a narrowly localized surface layer.[36] Thus, the method employed in the present work makes it possible to obtain simultaneously Mössbauer spectra from a 50 ± 10 mm thick layer located 300 nm from the surface as well as Mössbauer spectra from the interior of the sample by recording the γ-rays and characteristic x-rays.

3. CHARACTERISTICS OF MÖSSBAUER INVESTIGATIONS NEAR THE MAGNETIC-ORDERING TEMPERATURES

Mössbauer investigations are difficult to perform near the magnetic-ordering point, because in this temperature range the Zeeman lines in the spectrum often cannot be resolved, and this lowers substantially the accuracy with which the effective magnetic fields are determined. The situation is even more complicated if the iron ions in the crystal occupy several nonequivalent positions, as in Fe_3BO_6, since in the critical temperature range it is virtually impossible to distinguish lines referring to different sublattices. In the case of Fe_3BO_6, however, it was found that it is possible to decrease the number of observed spectral lines and thereby to increase the resolution. For this, a number of experimental possibilities and favorable circumstances, based on the crystallographic structure of Fe_3BO_6, were exploited: 1) the number of iron ions in the $8d$ and $4c$ positions and therefore the intensities of these lines are in the ratio 2:1; 2) the effective magnetic fields on the nuclei of $8d$ and $4c$ ions are different because the number of magnetic bonds of $8d$ and $4c$ iron ions is different and the quadrupole splittings of the lines in the sextuplets are substantial; and, 3) Fe_3BO_6 single crystals in which the a crystallographic axis is perpendicular to the plane of the plate were selected for the investigations. Therefore, near T_N the wave vector of the γ-rays was oriented in the direction of the effective magnetic fields, and for this reason the Zeeman-sextuplet lines corresponding to $\Delta m = 0$ transitions are missing in the absorption spectra. This improved the resolution of the spectra.

On the basis of what we have said above we inferred that the STRMS method and the favorable circumstances provided by the Fe_3BO_6 crystal will make it possible to investigate processes in a thin surface layer of a bulk sample near T_N and to obtain answers to the following questions:

1) Are the limits of the phase transition at the surface

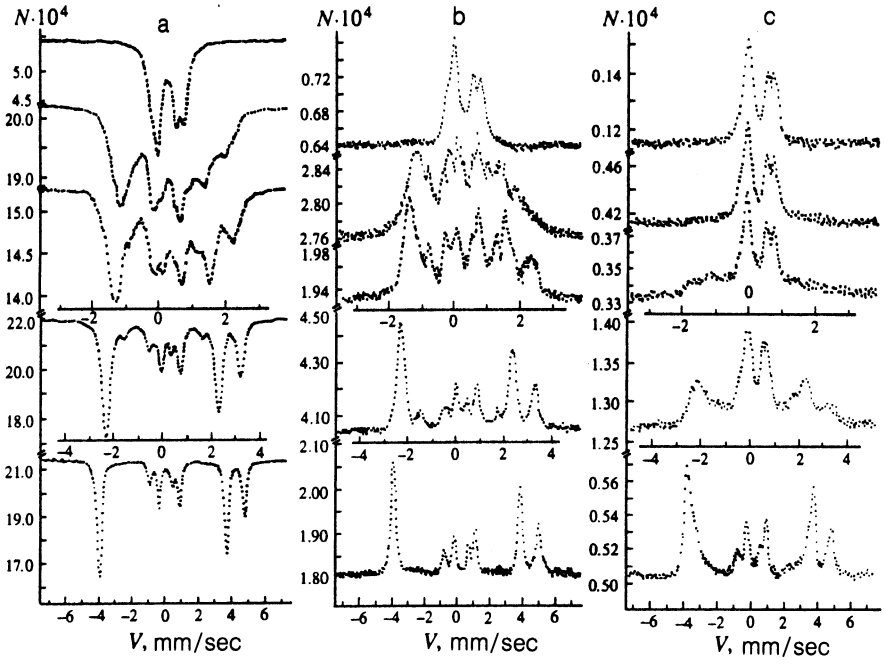

FIG. 2. Mössbauer spectra obtained for an Fe_3BO_6 crystal near T_N by recording γ-rays (a), x-rays (b), and electrons (c) at temperatures (bottom to top) of 471.2 K, 498.7 K, 503.7 K, 504.7 K, and 509 K.

different from the limits of this transition in the interior of the crystal?

2) Is the transition temperature at the surface different from that in the volume, i.e., does the paramagnetic transition occur at the same temperature or is this temperature shifted?

3) How do the phase transitions at the surface of a macroscopic crystal proceed?

4. RESULTS OF EXPERIMENTAL INVESTIGATIONS OF THE SURFACE AND INTERIOR OF Fe_3BO_6 MACROCRYSTALS NEAR THE NÉEL POINT

The Mössbauer spectra obtained by recording γ-rays, characteristic x-rays, and secondary electrons near the Néel point are a superposition of two Zeeman spectra corresponding to two nonequivalent positions $8d$ and $4c$ of iron ions. Some experimental spectra are displayed in Fig. 2. It is evident from the conventional Mössbauer spectra and the conversion x-ray Mössbauer spectra that up to $\sim$490 K the ratio of the line intensities of each Zeeman sextuplet are in the ratio 3:0:1:1:0:3. As the temperature increases further, the second and fifth lines (corresponding to transitions with $\Delta m=0$) of the sextuplet, which correspond to iron ions in the $4c$ positions, appear in the spectra. The second and fifth lines of the sextuplet, which belong to the iron ions occupying $8d$ positions, are not observed right up to $T_N-T=0.7$ K. The appearance of the lines belonging to iron ions in the $4c$ sublattice indicates that the magnetic moments deviate from the direction of the γ-ray beam. The causes of this phenomenon were explained in Ref. 27.

As the Fe_3BO_6 crystal is further heated through the Néel temperature the conventional Mössbauer spectra is transformed as follows: The splitting of the lines in the Zeeman sextuplet gradually decreases, and at T_N the lines collapse into a paramagnetic doublet. This restructuring of the spectra can be clearly seen in Fig. 2. Spectra in which Zeeman and paramagnetic lines are present simultaneously are observed in a very narrow temperature range near T_N.

It is evident from Fig. 2 that when the crystal is heated, lines similar to the lines of the paramagnetic phase appear in the conversion electron Mössbauer spectra superposed on the Zeeman sextuplet. The intensity of these lines increases with temperature, while the lines in the Zeeman sextuplet approach one another and their intensity decreases. At some temperature $T<T_N$ the Zeeman lines disappear. Thus the conversion electron Mössbauer spectra obtained near T_N are mixed spectra, i.e., the lines corresponding to the magnetically ordered state and the paramagnetic state coexist in them. As the crystal surface is approached, the paramagnetic lines become stronger and the Zeeman lines become weaker. This is seen clearly in the conversion electron Mössbauer spectra obtained from 50-nm-thick layers located at different depths from the crystal surface (Fig. 3).

Analysis of the experimental spectra obtained by recording radiation leaving layers at a depth L from the surface showed that the spectra can be divided into four groups corresponding to the following temperature ranges: 1) $T<T_W(L)$; 2) $T>T_N(L)$; 3) $T_M(L)<T<T_S(L)$; and, 4) $T_S(L)<T<T_N(L)$. The phase diagram is displayed in Fig. 4. The temperature dependence of the linewidths, obtained from the experimental spectra, is displayed in Fig. 5.

The spectra in the first region ($T<T_W(L)$) are a superposition of two Zeeman sextuplets corresponding to iron ions in nonequivalent $8d$ and $4c$ positions. The widths of all lines of the sextuplets are close to the natural widths, i.e., the crystal is in the magnetically ordered state Γ_M (Fig. 4).

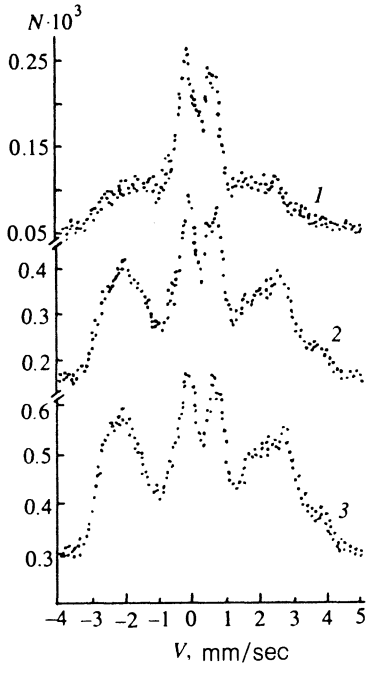

FIG. 3. Mössbauer spectra obtained near T_N by recording electrons from the layers *1*) 0–50 nm, *2*) 50–100 nm, and *3*) 150–200 nm in an Fe_3BO_6 crystal at $T=502.5$ K.

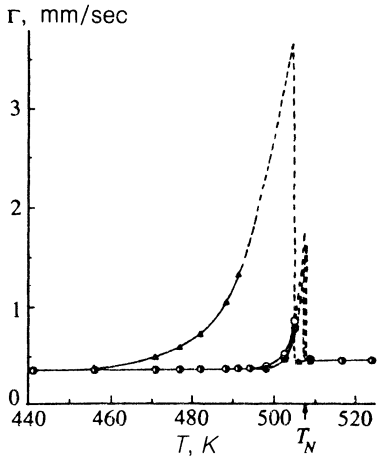

FIG. 5. Temperature dependence of the widths of the outer lines of the Mössbauer spectra obtained by recording γ-rays (○), x-rays (●), and conversion electrons (△).

In the second region ($T \geqslant T_N(L)$) the experimental spectra are a superposition of two quadrupole doublets corresponding to 8*d* and 4*c* positions of the iron ions. This means that the layers studied or the volume of the crystal in this temperature range are in the paramagnetic state Γ_P. Lines corresponding to the hyperfine Zeeman splitting are not observed in this phase.

In the temperature range from $T_W(L)$ to $T_S(L)$ the experimental Mössbauer spectra are similar to the spectra in the first region, with one exception. As the crystal is heated, starting at temperatures $T_W(L)$ the widths of the outer Zeeman-sextuplet lines corresponding to the transitions $\pm 3/2 \leftrightarrow \pm 1/2$ increase, and this broadening increases with the temperature (Fig. 5). The widths of the inner lines of the Zeeman sextuplets remain constant in this temperature range. This temperature range is designated as Γ_W in the phase diagram (Fig. 4).

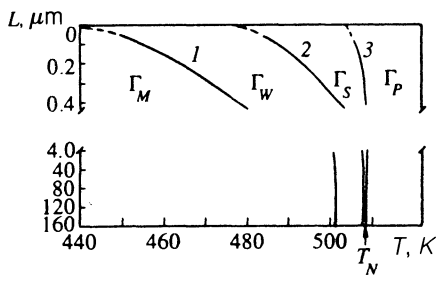

FIG. 4. Phase diagram near T_N: *1*—$T_W(L)$, *2*—$T_S(L)$, and *3*—$T_N(L)$.

The experimental spectra in the region $T_S(L) < T < T_N(L)$ (Fig. 2) are a superposition, on the Zeeman sextuplets, of lines whose positions coincide with the inner lines of the Zeeman sextuplet and resemble the paramagnetic doublets of the phase Γ_P. We designate this phase by Γ_S, and we term such spectra mixed. As the temperature increases from $T_S(L)$ up to $T_N(L)$, the outer lines of the Zeeman sextuplets become weaker and they disappear at $T_N(L)$. The inner lines of the sextuplet become stronger with increasing temperature from $T_S(L)$ to $T_N(L)$. As the temperature increases from $T_S(L)$ to $T_N(L)$ the widths of the outer lines increase and the widths of the inner lines remain constant (Fig. 5).

The phase diagram of the regions Γ_M, Γ_W, Γ_S, and Γ_P was obtained from the experimental spectra (Fig. 4). The limits of these regions were determined as follows: The position of the line $T_S(L)$ was found by extrapolating to zero the temperature dependence of the intensities of the inner (resembling paramagnetic) lines of the experimental spectra. The limit $T_W(L)$ is the temperature at which the outer Zeeman-sextuplet lines corresponding to the transitions $\pm 3/2 \leftrightarrow \pm 1/2$ start to broaden. The position of this limit was found from the temperature dependence of the widths of the outer lines of the sextuplets. The phase limit $T_N(L)$ was determined by the methods employed in Mössbauer spectroscopy for determining the Néel temperature:

1) The spectrum in which the Zeeman-splitting lines are missing and only quadrupole lines of the paramagnetic phase are observed was determined from the experimental spectra obtained in the region of the phase transition. The temperature at which the Zeeman lines disappear was taken as the Néel point.

2) The temperature-scanning method was used. In this method the temperature dependence of the number of photons recorded by the detector is determined (Fig. 6). The γ-ray source is stationary or moves with constant velocity. As one can see from Fig. 6, the number of photons recorded by the detector increases as $T_N(L)$ is approached

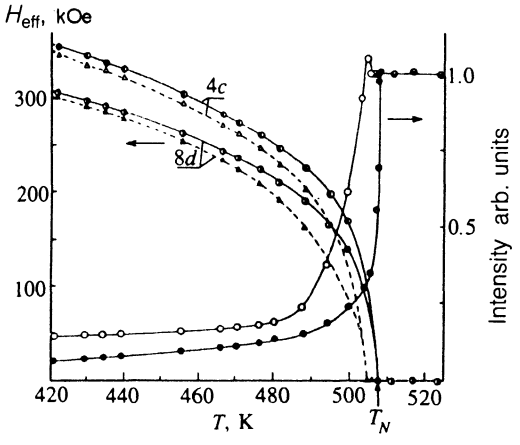

FIG. 6. Temperature dependence of the effective magnetic fields (○,△) and the number of recorded counts with "zero" velocity (●,○) for Fe_3BO_6, as determined from ordinary and conversion electron Mössbauer spectra, respectively. Identical results were obtained from ordinary and conversion x-ray Mössbauer spectra. The errors in determining the fields are smaller than the points.

from the low-temperature side. At the point $T_N(L)$ the curve saturates, and as the temperature increases further the number of photons recorded remains unchanged.

All methods gave the value of $T_N(L)$ with a spread of ± 0.2 K. It is evident from the phase diagram (Fig. 4) that the temperature range where mixed spectra are observed becomes wider as the surface is approached.

The parameters of the hyperfine interaction were determined from the experimental spectra. The temperature dependence of the effective magnetic fields obtained from the traditional Mössbauer and conversion electron Mössbauer spectra for the volume and surface of the Fe_3BO_6 crystal, respectively, is displayed in Fig. 6. As one can see from this figure, the effective magnetic fields at the nuclei of the iron ions located at the surface of the crystal decrease with increasing temperature more rapidly than the fields at the nuclei of iron ions located in the volume of the crystal. In order to check the reproducibility of the temperature results, many spectra were obtained and in different sequences on the temperature scale. Analysis of the data showed that the results obtained are reproducible.

5. ANALYSIS OF THE EXPERIMENTAL RESULTS

As one can see from the phase diagram displayed in Fig. 4, the regions Γ_W and Γ_S separate the paramagnetic state from the magnetically ordered state. As the crystal surface is approached, these regions become wider, the broadening occurring in the direction of low temperatures. Analysis of the spectra (Fig. 2) showed that as the temperature increases, the process of collapse of the Zeeman sextuplets in the conversion electron Mössbauer spectra differs from the process observed in conventional and conversion x-ray Mössbauer spectra.

A great deal of experimental work on Mössbauer investigations of magnetics near the Néel or Curie point has now been performed.[38] Narrow inner lines, which become stronger as T_N is approached, are observed superposed on the Zeeman lines with broadened outer lines in the Mössbauer spectra obtained at temperatures below the magnetic-ordering point. Such effects are observed in ultrasmall particles due to superparamagnetism phenomena. In this case, because the particles are smaller, the exchange interaction is weaker and becomes comparable to the thermal spin-excitation energy. As the thermal fluctuations become stronger, the relaxation time τ_S of the spin magnetic moments decreases to values comparable to the Larmor precession time of the nuclei that are responsible for the hyperfine structure of the spectrum observed in Mössbauer spectroscopy.

Investigation of the Mössbauer effect in paramagnetics (see Ref. 38 and the references cited there) showed that in the paramagnetic temperature range the Mössbauer spectra obtained in an external magnetic field have a relaxational character, and their structure depends on the external field and the temperature.

In the case of bulk magnetics analogous phenomena are observed near the Curie or Néel points. Such spectra appear because 1) some variation (temperature or field distribution) is present and 2) the spin magnetic moments relax with times comparable to the Larmor precession period τ_L of the Mössbauer nuclei.

In the first case the magnetic-ordering temperature at different points of the sample can be different due to fluctuations of the statistical distribution of the ions or due to formation of micrononuniformities. This is why paramagnetic and magnetically ordered phases coexist in some region near the transition temperature. The volume of a magnetic material can be imagined as being divided into a series of microscopic regions, resembling superparamagnetic particles, in each of which the magnetic moment fluctuates as a whole. These effects are observed in bulk materials in a narrow temperature range near the Néel point and depend on the technology employed for preparing the sample.

Critical superparamagnetism effects are unlikely to occur in the experimental Fe_3BO_6 crystals due to the presence of impurities and defects. This interpretation is refuted for the following reasons: 1) observations of mixed spectra in surface layers are not limited only to the critical region; 2) the region where mixed spectra are observed depends on how far away the layer is from the surface of the crystal; 3) no differences have been observed in investigations of crystals synthesized in different laboratories; and, 4) the crystals were processed by etching (as described in Sec. 2) three times, and the spectra obtained after each etching were identical.

The hyperfine structure of Mössbauer spectra under conditions such that the spins generating the magnetic field on the resonance nucleus relax is analyzed in many experimental and theoretical works. These phenomena have been described with the help of a quantum-mechanical perturbation model[39,40] as well as stochastic models.[41,42] Transitions between spin states of the ion are described as a function of time. Since the effective magnetic field (H_{eff}) at the nucleus of an Fe^{3+} ion is determined mainly by the

contact interaction of the spin magnetic moments, the shape of the Mössbauer spectrum depends on the behavior of the spins in the experimental sample, i.e., on the spin-fluctuation rate.

At low temperatures the spin-fluctuation time is significantly longer than the Larmor precession period of the nuclear spin ($\tau_S \gg \tau_L$), and the hyperfine Zeeman structure produced by the effective magnetic field is observed in the Mössbauer spectra in the form of a sextuplet, whose lines have the Lorentzian shape with natural widths (0.25–0.30 mm/sec). If, however, $\tau_L \gg \tau_S$, then the effective field H_{eff} is averaged to zero. The hyperfine Zeeman structure in the Mössbauer spectrum is not observed in this case, and the spectrum consists of lines of the paramagnetic doublet or singlet. Under certain conditions, however, it is possible to have $\tau_S \approx \tau_L$, and then lines resembling the lines of the paramagnetic state of the material are observed superposed on a spectrum having the hyperfine Zeeman structure. The spectra are then much more complicated, because every spin moment can produce its own characteristic field (H_{eff}) at a nucleus, it can have its own hyperfine structure, and it can fluctuate with its own relaxation time.

Thus the best explanation of the Mössbauer spectra observed in Fe_3BO_6 near T_N is as follows. The spectra under discussion were obtained by recording secondary electrons, arising from $\sim$50 nm thick layers. It is obvious from the experimental spectra that the paramagnetic transition temperatures $T_N(L)$ are different in these layers and depend on the depth L of the layer from the surface. Evidently, this thickness is too large to talk about a single value of $T_N(L)$ for this layer, and the layer can be represented as a series of thinner layers in which the paramagnetic transition temperature $T_N(L)$ decreases as the surface is approached (naturally, this partitioning cannot be infinite.) Therefore, the experimental Mössbauer spectra are a superposition of spectra from thin layers, whose ordering temperatures depend on the depth L of the layer from the surface. It is evident from the experimental spectra that in the region Γ_W the outer lines broaden asymmetrically, and this asymmetry, directed toward the center of the spectrum, increase with the temperature of the crystal. The results obtained by analyzing these spectra showed that they are described best in the case when the theoretical spectrum is given in the form of a collection of spectra with different H_{eff}. Such a collection of values of H_{eff} can exist only if there exists a collection of Néel temperatures.

A collection of spectra with different H_{eff} was likewise employed in the region Γ_S at temperatures close to the limit $T_S(L)$ in order to describe the experimental spectra theoretically. However, the spectra with the lowest values of H_{eff} in this collection should have, in this case, a relaxational form, i.e., strong central lines should be observed on top of broadened outer lines. The experimental spectra obtained in the same region Γ_S but closer to the phase limit $T_N(L)$ are described best by the above collection of spectra supplemented by lines corresponding to the paramagnetic phase Γ_P. The contribution of Γ_P-phase lines arises from paramagnetic outer layers of the crystal surface. This is proved by the spectra obtained by recording secondary electrons from layers located at different depths from the crystal surface (Fig. 3). It is evident from these spectra that the paramagnetic-phase fraction increases as the crystal surface is approached.

Near the Néel point the surface layer of the Fe_3BO_6 crystal can apparently be divided into a series of thin layers. Each layer has its own paramagnetic transition temperature $T_N(L)$ and its own spin-moment relaxation time $\tau_S(L)$, comparable to the Larmor precession period, and these quantities depend on the depth L of the layer from the surface. Within each layer, as the temperature increases, the spin relaxation time changes from the maximum value, which occurs at the temperature $T_S(L)$, to the minimum value, which occurs at the paramagnetic transition temperature $T_N(L)$.

Thus the spectra observed in the surface layers of the Fe_3BO_6 crystal near T_N appear mainly due to increased fluctuations of the spin magnetic moments and a decrease of the magnetic-ordering temperature as the surface is approached. Since some of the magnetic bonds of the iron ion are missing directly on the crystal surface, the exchange interaction is weakened and this in turn could be why the fluctuations of the spin moments are stronger and the ordering temperature is lower at the surface. As the temperature increases, this process of breaking magnetic bonds propagates into the crystal because the upper layers are the first layers to pass into the paramagnetic state.

On the basis of the experimental results the paramagnetic transition in a macroscopic crystal can be described as follows. As the bulk Fe_3BO_6 sample is heated, the rate of fluctuations of the spin magnetic moments of the iron ions located at the surface of the crystal increases, and paramagnetic regions appear at the surface, and at temperatures below T_N for the volume of the crystal. As the temperature of the sample increases further, the paramagnetic phase spreads along the surface and at the same time penetrates into the crystal. Further, at the Néel temperature the thermal energy destroys the magnetic ordering simultaneously in the entire remaining volume of the crystal. When magnetic order in the sample is destroyed, relaxation of the spin magnetic moments is observed in a very narrow temperature range near T_N. The crystal contains a surface layer with some critical thickness, where both the spin relaxation time and the transition temperature $T_N(L)$ change. In layers located at depths greater than the critical thickness the paramagnetic transition occurs at a temperature corresponding to T_N for the interior of the crystal. At temperatures ranging from $T_N(L)$ to T_N in the crystal the matter in the interior is in a magnetically ordered state, while the surface of the sample is in a paramagnetic state.

6. CONCLUSIONS

Our investigations of the behavior of the magnetic system near T_N in Fe_3BO_6 simultaneously in layers at the surface, near the surface, and in the volume of the crystal revealed the following:

1) At the surface of the crystal the paramagnetic transition occurs at temperatures $T_N(L)$ below the Néel point T_N at which the transition is observed in the interior of the

crystal. The temperature $T_N(L)$ of the transition into the disordered state for a thin layer located at a depth L from the surface of the crystal decreases as this layer approaches the surface.

2) The transition of the surface to the paramagnetic state is preceded by a wide temperature range in which relaxational processes are observed. In the interior of the crystal relaxational phenomena occur in a very narrow temperature range. The temperature range where relaxational processes are observed becomes narrower as the distance from the surface increases.

3) Near T_N there exists a nonuniform state when the crystal is magnetically ordered in the interior but the surface of the crystal is disordered. Between the magnetically ordered volume of the crystal and the disordered surface layer there exists a transitional region which expands as the crystal surface is approached.

On the basis of the results obtained it is inferred that there exists a surface layer with critical thickness where the paramagnetic transition temperature changes from some minimum value (at the surface) up to T_N (at the lower boundary of this critical layer). In the layer located at a distance from the crystal surface greater than the critical thickness, the magnetically ordered state remains right up to T_N.

[1] M. I. Kaganov and A. V. Chubykov in *The Magnetic Properties of Crystalline and Amorphous Media* [in Russian], Nauka, Novosibirsk, 1989, p. 135.
[2] T. Kaneyoshi, J. Phys. Condens. Matter **3**, 4497 (1991).
[3] J. Mathon, Rep. Progr. Phys. **51**, 1 (1988).
[4] U. Gradmann, J. Magn. Magn. Mater. **100**, 481 (1991).
[5] T. Shinjo, Surf. Sci. Rep. **12**, 49 (1991).
[6] M. I. Kaganov and A. M. Omel'yanchuk, Zh. Eksp. Teor. Fiz. **61**, 1679 (1971) [Sov. Phys. JETP **34**, 895 (1974)].
[7] M. I. Kaganov, Zh. Eksp. Teor. Fiz. **62**, 1196 (1972) [Sov. Phys. JETP **35**, 631 (1972)].
[8] D. Mills, Phys. Rev. B **3**, 3887 (1971).
[9] M. I. Kaganov and N. S. Karpinskaya, Zh. Eksp. Teor. Fiz. **76**, 2143 (1979) [Sov. Phys. JETP **49**, 1083 (1979)].
[10] N. S. Karpinskaya, Fiz. Tverd. Tela **21**, 1160 (1979) [Sov. Phys. Solid State **21**, 672 (1979)].
[11] C. Rau, Phys. Rev. Lett. **58**, 2714 (1987).
[12] C. Rau, Appl. Phys. A **49**, 579 (1989).
[13] C. Rau *et al.*, J. de Phys. **49**, C8-1627 (1988).
[14] D. Weller, S. F. Alvarado, W. Guhar *et al.*, Phys. Rev. Lett. **54**, 1555 (1985).
[15] G. Lugert and G. Bayreuther, Phys. Rev. B **38**, 11068 (1988).
[16] M. Przybylski and U. Gradmann, Phys. Rev. Lett. **59**, 1152 (1987); M. Przybylski and J. Korecki, Hyperfine Interactions **57**, 1152 (1987).
[17] J. C. Walker, R. Droste, G. Stern, and F. Tyson, J. Appl. Phys. **55**, 2500 (1984).
[18] A. Ochi, K. Watanabe, M. Kiyama *et al.*, J. Phys. Soc. Jpn. **30**, 2777 (1981).
[19] R. D. McGrath, R. M. Mitzabayer, and F. C. Walker, Phys. Lett. A **67**, 149 (1978).
[20] P. P. Kovalenko, V. G. Labushkin, E. R. Sarkisov, and I. G. Talpenin, Fiz. Tverd. Tela **29**, 593 (1987) [Sov. Phys. Solid State **29**, 340 (1987)].
[21] J. G. White, A. Miller, and R. E. Nielsen, Acta Cryst. **19**, 1060 (1965).
[22] R. Wolfe, K. D. Pierce, M. Eibschutz, and J. W. Nielsen, Solid State Commun. **7**, 949 (1969).
[23] O. A. Bayukov, V. P. Ikonnikov, and M. P. Petrov in *Proceedings of the International Conference on Magnetism* [in Russian], Moscow, 1973, Vol. 3, p. 313.
[24] A. S. Kamzin, V. A. Bokov, and M. K. Chizhov, Fiz. Tverd. Tela **18**, 2795 (1976) [Sov. Phys. Solid State **18**, 1631 (1976)].
[25] A. S. Kamzin and V. A. Bokov, Fiz. Tverd. Tela **19**, 2131 (1977) [Sov. Phys. Solid State **19**, 1247 (1977)].
[26] A. S. Kamzin and L. A. Grigor'ev, Pis'ma Zh. Eksp. Teor. Fiz. **57**, 543 (1993) [JETP Lett. **57**, 557 (1993)]; A. S. Kamzin and L. A. Grigor'ev, Zh. Eksp. Teor. Fiz. **104**, 3489 (1993) [Sov. Phys. JETP **77**, 658 (1993)].
[27] A. S. Kamzin and V. A. Bokov, Fiz. Tverd. Tela **19**, 2030 (1977) [Sov. Phys. Solid State **19**, 1187 (1977)].
[28] A. L. Irshinskii and V. M. Cherepanov, Zh. Eksp. Teor. Fiz. **79**, 1412 (1980) [Sov. Phys. JETP **52**, 714 (1980)].
[29] C. Voigt and W. Roos, J. Phys. C: Solid State Phys. **9**, 1409 (1976).
[30] A. S. Kamzin and L. A. Grigor'ev, JETP Lett. **27**, 477 (1978).
[31] A. I. Sokolov, JETP Lett. **27**, 480 (1978).
[32] J. Pollman *et al.*, *Hyperfine Interactions* (1994). *Proceedings of the International Conference on Application Mossbauer Spectroscopy*, Canada, 1993.
[33] A. S. Kamzin, V. P. Rusakov, and L. A. Grigoriev in *Proceedings of the International Conference on Physics of Transition Metals*, Naukova dumka, Kiev, 1988, Part 2, p. 271.
[34] A. S. Kamzin and L. A. Grigor'ev, Pis'ma Zh. Tekh. Fiz. **16**, 38 (1990); A. S. Kamzin and L. A. Grigor'ev, Prib. Tekh. Eksp., No. 2, 74 (1991).
[35] A. S. Kamzin, S. M. Irkaev, Yu. N. Mal'tsev, and L. A. Grigor'ev, Prib. Tekh. Eksp., No. 1, 80 (1993).
[36] A. S. Kamzin and L. A. Grigor'ev, Pis'ma Zh. Tekh. Fiz. **19**, 50 (1993); A. S. Kamzin and L. A. Grigor'ev, Pis'ma Zh. Tekh. Fiz. **19**, 32 (1993).
[37] A. I. Chumakov and G. V. Smirnov, Zh. Eksp. Teor. Fiz. **89**, 1819 (1985) [Sov. Phys. JETP **62**, 1044 (1985)].
[38] I. P. Suzdalev, *Dynamic Effects in Mossbauer Spectroscopy* [in Russian], Atomizdat, Moscow, 1979.
[39] A. M. Afanas'ev and Yu. Kagan, Zh. Eksp. Teor. Fiz. **45**, 1660 (1963) [Sov. Phys. JETP **18**, 1139 (1964)].
[40] A. M. Afanas'ev and V. D. Gorobchenko, Zh. Eksp. Teor. Fiz. **66**, 1406 (1974) [Sov. Phys. JETP **39**, 690 (1974)].
[41] M. Blume, Phys. Rev. Lett. **14**, 96 (1965).
[42] Van der Woude and A. J. Dekker, Phys. State Solids **9**, 775 (1965).

Translated by M. E. Alferieff